Biophysical Chemistry 28 (1987) 235–244
Elsevier

BPC 01202

Reconstruction of NOESY maps

A requirement for a reliable conformational analysis of biomolecules using 2D NMR

Dominique Marion, Monique Genest and Marius Ptak

Centre de Biophysique Moléculaire (C.N.R.S.) and Université d'Orléans, 1A, Ave de la Recherche Scientifique, F-45071 Orléans Cedex 2, France

Received 22 April 1987
Revised manuscript received 21 September 1987
Accepted 30 September 1987

Nuclear Overhauser effect; Conformational analysis; 2D NMR; Molecular model; Lipopeptide; Spin diffusion

The modelling of the conformation of a biomolecule in solution is based mainly on the internuclear distances deduced from measurements of nuclear Overhauser effects (nOe) in NOESY correlation maps. The distances are then used as restraints in the energy minimization procedure, which leads to one or several optimized conformations. A general and safe technique for validating these structures with respect to the experimental data is here proposed: from the internuclear distances, the relaxation matrix can be computed under the assumption of a unique rotational correlation time. By stepwise integration of these relaxation equations, the NOESY maps can be accurately reconstructed for any mixing time. Because multi-spin effects are correctly taken into account, any difference between the experimental and theoretical maps can be easily interpreted in terms of conformation, and possible inconsistencies due to conformational averaging can be pointed out. The technique is illustrated for a bacterial lipopeptide, mycosubtilin, the spectrum of which is completely assigned.

1. Introduction

Two-dimensional (2D) NMR has proven to be one of the most powerful techniques for determining the constitutions, conformations and interactions of biological macromolecules of medium size in solution [1–6]. These determinations rely on spin connectivies corresponding to scalar and dipolar interactions. The modelling of a conformation is generally started using a set of internuclear distances deduced from the nuclear Overhauser effects (nOe). Some complementary constraints can be provided by converting the ^3J coupling constants into dihedral angles through a Karplus-like relationship. The conversion of an nOe into an internuclear distance can be directly achieved only for an isolated two-spin system by comparison with a reference: this latter can be provided by any two-spin system of known interproton distance exhibiting the same motional properties. However, for biological molecules, one encounters several difficulties with nOe quantitative interpretation because of multi-spin effects and intramolecular motions.

With respect to multi-spin effects [7], restriction to short mixing times constitutes a sound precaution as long as the strongest nOes suffice for characterization of the molecular topology. In this way, discrimination between quite distinct stereo-

Correspondence (present) address: D. Marion, National Institutes of Health, National Institute of Diabetes and Digestive and Kidney Diseases, Laboratory of Chemical Physics, Bethesda, MD 20892, U.S.A.

regular structures (β-sheets and α-helices in proteins, for example) is straightforward [8], even on the basis of qualitative data. Indeed, in this case, the set of data exhibits a high confidence level: the nOes are not only strong but also redundant. Accordingly, the overall topology of the refined structure obtained by optimization can never differ in all respects from that of the initial one, because optimization algorithms tend to converge towards the nearest local minimum. Let us finally remark that the main validation for the occurrence of stereoregular features in refined structures is the great likelihood of the existence of such features, a relatively subjective criterion.

In peptide studies, long-range nOes may be of the utmost importance for correctly defining the molecular topology. In such cases, where all nOes are taken into account, one has to tackle the problem of spin diffusion, long-range nOes being detectable only at longer mixing times. As a result of the relative positions of the interacting nuclei, multi-spin effects can be accurately computed in different ways [18], under the assumption of a rigid molecule characterized by a unique rotational correlation time. Refinement of the starting model of the conformation relies on minimization of the intramolecular energy subject to several geometrical constraints (from nOe and/or ^3J). In the course of the refinement, the conformation is modified several times either by the minimizer or manually. Among all the spin pairs in a biological molecule, only a few will be close enough ($d <$ 4–5Å) to give rise to NOESY cross-peaks, whereas no peaks will be observed for the others. Because the information content of the set of absent nOes is quite poor, their omission from the minimization is safe: indeed, they could overwhelm the less abundant, but more reliable short-range information. However, one has to check the refined structure afterwards to ensure that the distances corresponding to the omitted pairs are all larger than a given threshold, determined by the signal-to-noise ratio of the experimental data.

For this purpose, we find that one of the most efficient ways for fitting the conformational and spectral parameters relies on comparison of the experimental NOESY with a reconstructed NOESY map in which nOes are computed from the spatial arrangement of the interacting spins. Using the analytical power of the human eyes, this visual correspondence allows a direct evaluation of the validity of the model with respect to the true conformation and points out possible aberrations due to causes other than multi-spin effects. The technique is illustrated here on mycosubtilin, a bacterial lipopeptide under investigation in our laboratory, which is small enough to allow a complete resonance assignment of the peptide part and then the complete reconstruction of the NOESY map.

2. Materials and methods

Mycosubtilin [9,10], an antifungal lipopeptide from *Bacillus subtilis*, has the following sequence: cyclo(Asn-D-Tyr-D-Asn-Gln-Pro-D-Ser-Asn-Xaa) where Xaa denotes a β amino acid carrying a long hydrophobic tail. This lipopeptide was kindly provided by Drs F. Peypoux and G. Michel (University of Lyons I, France) as described elsewhere [9].

^{1}H-NMR measurements were recorded on a Bruker AM 300 WB instrument (^{1}H = 300 MHz). NOESY spectra [11] without randomization of the mixing time were recorded with time-proportional phase increments (TPPI) in both directions [12]. The 256×4096 sampled data matrix was then Fourier transformed into a 512×4096 absorption mode map. The spectra were recorded in pyridine-d_5 at low temperature ($-20\,^\circ$C) in order to slow down the molecular tumbling and thus observe sizeable nOes. The assignment of mycosubtilin ^{1}H-NMR resonances (by means of the well-known COSY-NOESY technique) has been previously reported [10].

For internuclear distance measurements, a series of NOESY spectra (with mixing times ranging from 40 to 450 ms) were measured. A preliminary rough estimate of the interproton distances is derived from the initial slope of the build-up curve and a confidence interval is defined, based mainly on the corresponding signal-to-noise ratio of each cross-peak. Refinement of the conformation is performed using a main-frame computer program written for this purpose, described in detail elsewhere [13]. The conformation is first optimized

with respect to the spectral parameters (nOe and ^3J couplings) and with additional semi-empirical energy criteria.

The NOESY map reconstruction is performed on a microcomputer, by using the coordinates of the structure. The computer used for this study is an Olivetti M 24, and MS-DOS machine with 640K memory, an 8086 processor and an 8087 floating-point coprocessor. With the Fortran program based on the theory described below, a typical running time is about a few minutes for one integration step on a molecule containing 60 protons. The accuracy of the computed nOe values is determined primarily by the accuracy of the atomic coordinates given as input (roughly 1–2%) rather than by truncation errors during the matrix multiplication performed on 64-bit real data.

3. Theory

In an N-spin system, cross relaxation of the longitudinal magnetization proceeds according to [11, 14]:

$$\frac{\mathrm{d}}{\mathrm{d}t}\boldsymbol{M} = -\boldsymbol{R}\boldsymbol{M} \tag{1}$$

where the vector $\boldsymbol{M}$ comprises the deviation of the longitudinal magnetizations M_{zk} from thermal equilibrium. Assuming purely dipolar relaxation, the diagonal terms of the relaxation rate matrix $\boldsymbol{R}$ are given by:

$$R_{ii} = \sum_{i \neq j} \rho_{ij} = K \sum_{i \neq j} \frac{1}{r_{ij}^6} (3J(\omega) + J(0) + 6J(2\omega)) \tag{2}$$

and the off-diagonal terms by:

$$R_{ij} = \sigma_{ij} = K \frac{1}{r_{ij}^6} (6J(2\omega) - J(0)) \tag{3}$$

where $J(\Omega)$ $(\Omega = 0, \omega, 2\omega)$ denotes the spectral density at multiple values of the spin Larmor frequencies.

The main problem in calculating a relaxation rate is in essence that of determining the appropriate spectral density function. This is simplest when dealing with rigid molecules undergoing isotropic rotational Brownian motion. Unfortunately, unless the conformation of the molecule is provided independently by other physical methods, the information contained in relaxation data cannot reveal the possible presence of multiple and/or anisotropic motion.

Only when the rigid isotropic model fails does the calculation warrant further complication by including either an internal motion [15] or an anisotropy of the overall tumbling [16]. The present approach can be easily adapted for rod-like molecules (such as moderately long oligonucleotides) in which the orientation of each internuclear vector with respect to the principal axes of the molecular diffusion frame [17] is known.

In contrast, the handling of an internal motion is trickier: it requires a secure knowledge not only of the motional characteristics of each spin, but also of the correlation between the motions. Therefore, the failure of the rigid molecule assumption will be analyzed later only qualitatively in terms of 'averaged distances'.

According to Macura and Ernst [11], the integrated intensity of a peak at (f_i, f_j) in the NOESY spectrum depends upon the mixing time t_m:

$$a_{ij}(t_m) = \sum_k [\exp(-\boldsymbol{R}t_m)]_{ik} a_{kj}(0) \tag{4}$$

For sufficiently short mixing time, the matrix exponential can be replaced by:

$$a_{ij}(t_m) = \sum_k (\delta_{ik} - R_{ik}t_m) a_{kj}(0) \tag{5}$$

or in a matrix form:

$$\boldsymbol{A}(t_m) = (\delta - \boldsymbol{R}t_m)\boldsymbol{A}(0) \tag{6}$$

For longer mixing times, the intensities can be obtained in an iterative manner by splitting the mixing times into sufficiently short intervals:

$$\boldsymbol{A}(t_m + t) = (\delta - \boldsymbol{R}t)\boldsymbol{A}(t_m) \tag{7}$$

Keepers and James [18] have used an alternative approach to compute integrated NOESY intensities. Instead of the stepwise integration proposed here, the relaxation rate matrix, $\boldsymbol{R}$, whose ele-

ments establish the intensities, is diagonalized using a numerical procedure. While this approach has proven to be efficient and numerically stable on their test runs for three- and four-spin systems, our present technique has two major advantages. Firstly, it gives a better feeling for the spin-diffusion paths; and secondly, it is relatively faster:

The integration technique obviously requires the computation of nOes at intermediate times which enables one to assign the relay involved in spin diffusion. This analysis cannot be accomplished using diagonalization for lack of a direct assignment of a given eigenvalue to an individual spin pair.

Furthermore, our technique, which does not rely on the convergence of a diagonalization procedure (whether it is Jacobi's method or a derived one through a tridiagonal matrix), is slightly faster for the same yield of information. On an N-spin system, a complete build-up curve with M intermediate values is a workload of about $2 \times M \times N^3$ individual operations with either technique, but the eigenvalues and vectors must be provided first for the method of Keepers and James (an additional $6 \times N^3 - 20 \times N^3$ operations) [19].

In order to compute the nOe intensities, an estimate of the rotational correlation time is required. For this purpose, one can make use not only of the initial build-up rate of the Hβ-Hβ' cross-peak but also of the differential time behavior of their cross-peaks with a third nucleus H^x. Indeed, because of the short Hβ-Hβ' distance, this pair can efficiently transfer from H^x to Hβ via Hβ' and vice versa, irrespective of the actual geometry of the three-spin system. Thus, whatever the chosen mixing time, a more marked difference between the intensities of H^x-Hβ and H^x-Hβ' peaks is observed over all residues for faster molecular motion relative to slower motion. This finding prompted us to compare the experimental data with several NOESY maps simulated with various correlation times, and led us to the conclusion that 1.6 ns is the best compromise. No significant scattering was detected between the various side chains, even though they are more or less tightly stabilized by intramolecular hydrogen bonds.

In the computed maps shown in section 4, the cross-peaks are depicted as simple circles, with a diameter directly proportional to the nOe. Consequently, one disregards several features which could contribute in a very complex manner to the shape of the cross-peaks (experimental linewidth, multiplet pattern due to ^3J couplings, bad digital resolution along the ω_1 direction). In the later discussion, the computed nOe effects are compared with the corresponding NOESY intensities (but not with the 2D integrals of the cross-peaks) under the assumption, almost always satisfied, that the other parameters contribute to the line shape in a similar manner for all the various cross-peaks compared. So far, to minimize computing time, a more rigorous approach has not been implemented to incorporate the lineshape contributions: as regards other uncertainties (motion, phasing, ...), the improvement brought about could be meaningless for the derived conformation.

4. Results and discussion

Using the previously reported assignment of ^{1}H resonances in mycosubtilin [10], all NOESY cross-peaks can be identified. Fig. 1 displays a blow-up of the NOESY spectrum recorded at $-20\,^\circ$C (mixing time 125 ms). The lowest contour level has been intentionally chosen not too close to the noise level in order to ensure a comfortable level of confidence in each observed cross-peak.

The choice of mixing time for the derivation of distance results from a compromise between two opposing sources of error, one arising from the nOe quantification, the other from their conversion into distances. Because the experimental noise in a 2D map includes one contribution directly proportional to the diagonal peaks ('t_1' noise), the cross-peaks should reach a minimum level relative to the diagonal: consequently, very short mixing times (say < 50 ms) are not suitable. Longer mixing times provide better estimates of the NOESY intensities but one has to tackle the multi-spin effects to convert them into distance.

Fig. 2 shows the simulation of the nOe build-up for several spin pairs near D-Tyr 2 as depicted in the structure S4 discussed below. Even over this

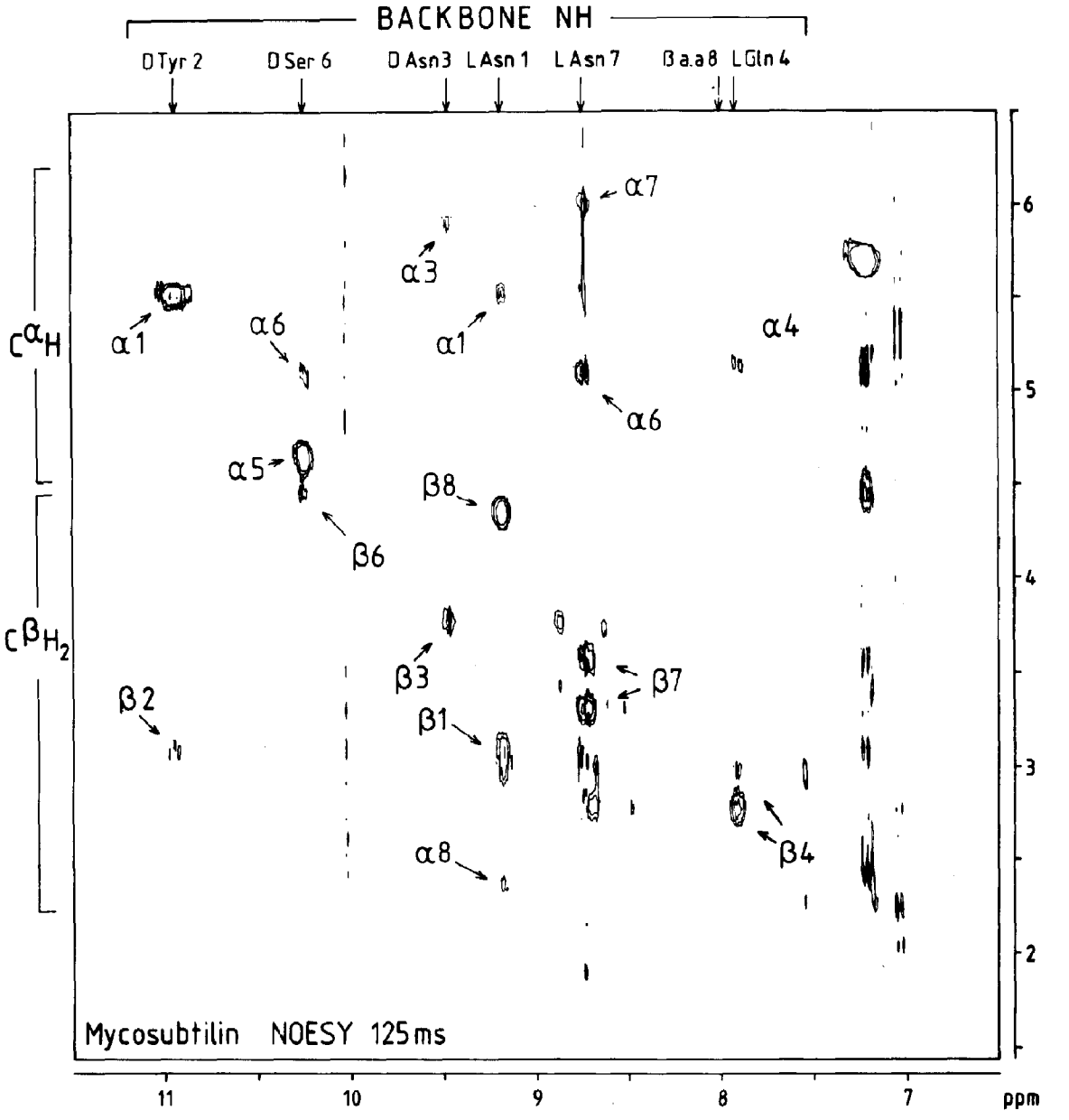

Fig. 1. Experimental NOESY map of mycosubtilin recorded at −20 °C with 125 ms mixing time (no random variation) displayed in the absorption mode. The connectivities between the NH of the backbone and the $C^{\alpha}H$, $C^{\beta}H$... are assigned. Except for those in the column at $\omega_2 = 7.2$ ppm (the $C_{2,6}$ protons of D-Tyr 2), all unassigned peaks correspond to cross-peaks involving the amide protons of the side chains and are not discussed here.

limited range of mixing times (0–125 ms), the curves are highly non-linear. As in any peptide residue, the short Hβ-Hβ distance is the keystone to the multi-spin effects. First, the Hβ^1-Hβ^2 curve (◆) is no longer linear after 50 ms. Concurrently, the NH-Hβ^2 curve (○) bends upward as a conse-

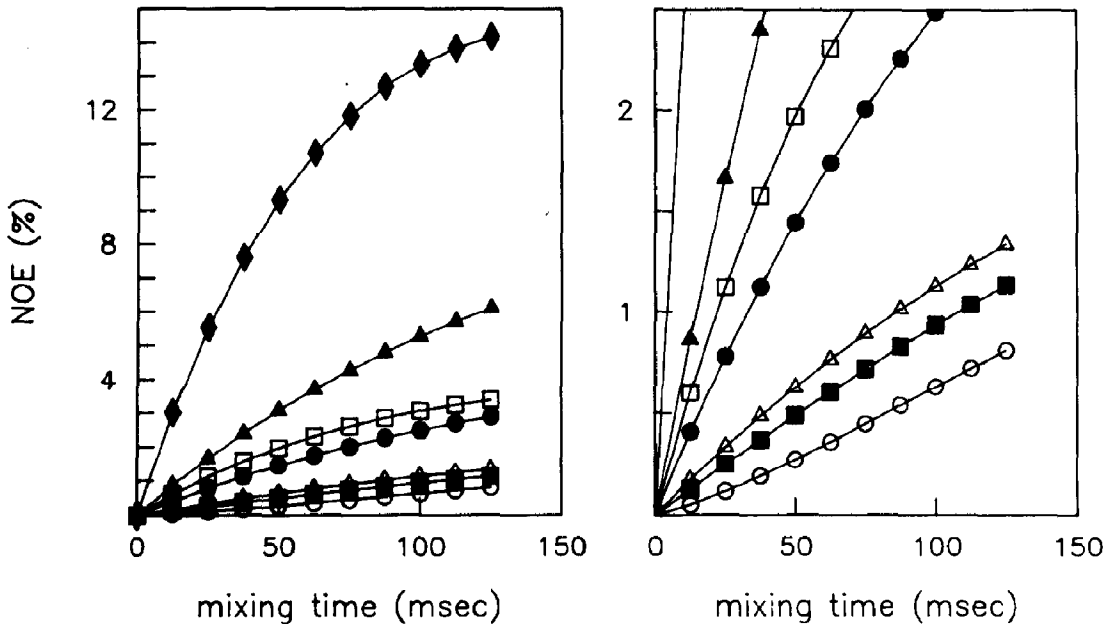

Fig. 2. Nuclear Overhauser effect build-up curves for various spin pairs in the surroundings of D-Tyr 2. The right-hand panel depicts the data in the left-hand panel on an expanded scale, in order to manage the different magnitudes of the effects. The percentages (given below in front of the symbols) indicate the under- (−) or overestimation (+) of the computed nOe effects, if multi-spin effects are neglected (initial rate approximation). Intraresidue nOe (D-Tyr 2–D-Tyr 2): (○) NH-Hβ^2 (−39%), (□) NH-Hβ^1 (+76%), (◆) Hβ^1-Hβ^2 (+110%), (△) NH-Hα (+28%), (●) Hα-Hβ^2 (+40%), (■) Hα-Hβ^1 (+8%). Interresidue nOe (L-Asn 1–D-Tyr 2): (▲) Hα-NH (+41%).

quence of the sharp build-up of NH-Hβ^1 (□). Had one disregarded the multi-spin effects, the NH-Hβ^2 would be underestimated by almost 40%. This trend becomes more pronounced for longer mixing times: however, no additional peak has been experimentally observed in these maps (see figures in ref. 20). Because of the decay of the diagonal peaks and thus of the t_1 noise, they look better, but the distance determination is less accurate due to spin diffusion.

The peaks assigned in fig. 1 all involve a backbone NH: they are very important for characterizing the local conformation, but are likely to be affected by multi-spin effects because of the compactness of cyclic peptides. Rough initial estimates of the shortest distances (< 3.5 Å) are obtained by quantifying the intensities in this NOESY map. One purpose of the iterative process (structure optimization and NOESY reconstruction) is to check for inconsistencies in the initial distance estimates.

Once the first optimized conformation has been obtained, the coordinates of this structure are used to compute first the internuclear distances, and then the integrated cross-peak intensities. The only additional knowledge required for this latter step is a reliable value for the correlation time of the molecular motion. The search for the best conformation with respect to NOESY data is thus achieved iteratively in the following manner. At each step, comparison of the theoretical map with the experimental one allows both a qualitative and quantitative improvement of the distance data set used in the subsequent steps. The previous distance estimates are corrected while the number of pieces of information can be increased by extending to larger distances, i.e., to weaker NOESY peaks.

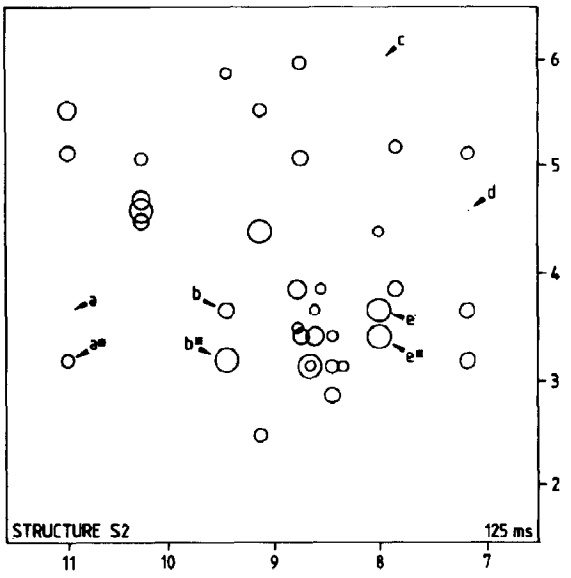

Fig. 3. Computed theoretical map corresponding to structure S2 (mixing time, 125 ms; correlation time of the molecular tumbling chosen as equal to 1.6 ns). The labelled peaks and their conformational relevance are discussed in the text.

This procedure is better illustrated by two examples: let us compare the experimental map displayed in fig. 1 with two computed ones respectively shown in figs. 3 and 4. Both correspond to an already partially optimized structure after several optimization-reconstruction cycles. The two structures originate from two runs including energetical optimization: S4 is the result of a completely restrained optimization (^3J and nOe) (fig. 4), whereas S2 (fig. 3) is obtained by letting distance constraints prevail over that of ^3J.

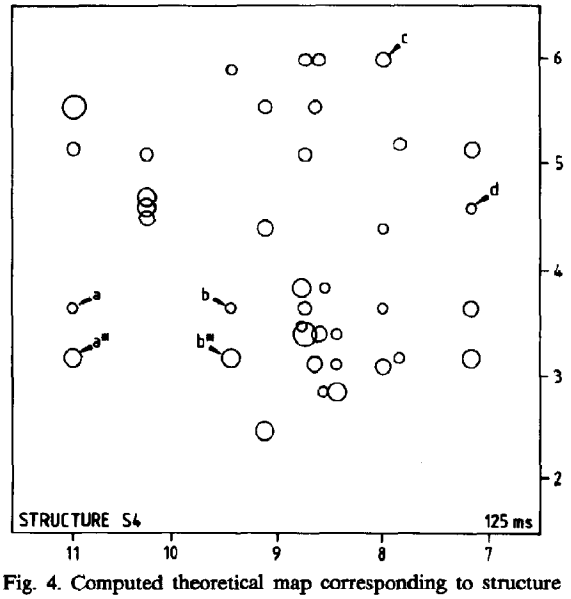

Fig. 4. Computed theoretical map corresponding to structure S4 (see fig. 3)

The complete description of the conformation of mycosubtilin, which is not the major aim of this paper, is reported elsewhere [20]. However, we shall discuss here three interesting details of figs. 3 and 4, as well as their conformational relevance.

4.1 Conformation of the D-Tyr 2 side chain

During the following discussion of this local feature, one has to bear in mind what information has or has not been used in the runs leading to S2 and S4: the long-range constraints between the D-Tyr 2 ring and the side chain of D-Ser-6 (see below) have been included, but all data involving the Hβ of D-Tyr 2 have been omitted for lack of stereospecific assignment. We shall demonstrate that two interrelated ambiguities relevant to this side chain can be solved at once: the Hβ assignments and rotation around the C^α–C^β bond.

The two usual ways of interpreting the ^3J Hα-Hβ (10 Hz at $\delta = 3.3$ ppm and 4.6 Hz at $\delta = 3.7$ ppm) assume either a unique rotamer or the average of the three staggered rotamers (Pachler approach [21]). Among the six conformers in 60° steps, the staggered ones (-60, 60 and 180°) are more favorable energetically than the others. At first glance, the experimental ^3J could fit two unfavorable ones ($\chi_1 = 0$ or $-120°$) but, regardless of the Hβ assignment, disagreements in the simulated maps still remain. In the first case ($\chi_1 = 0°$), one Hβ is close to the NH of D-Asn 3 but neither Hβ exhibits a sizeable connectivity to its own NH (as in fig. 1). In the second case, the smaller nOe with the NH of D-Tyr 2 corresponds to the wrong Hβ with the large coupling. As expected, these less favorable rotamers with regard to energy are ruled out on experimental grounds.

Let us now compare the experimental (fig. 1) map with those computed for the S2 and S4

structures (figs. 3 and 4), in which χ_1 is set to 60°. The rough agreement of the relative intensities of cross-peaks a and a* (a* > a), in conjunction with the ^3J values, leads to the following two conclusions: the low-field proton is Hβ^2 and the predominant rotamer has $\chi_1 = 60°$. As far as the assignment is concerned, this result is in full agreement with the work of Kobayashi et al. [22], who have studied stereoselectively β-deuterated species of Ac-L-Tyr-NH-Me.

However, it turns out that a single conformation is not able to account for the complete set of data (^3J and nOe). This is supported by the Pachler interpretation of the ^3J, which actually leads to only 60–70% occurrence of $\chi_1 = 60°$ (and 15–20% for each of the other two). Using a ratio of 60 : 20 : 20 weighting, we computed the average of the three corresponding simulated maps and compared the results with the experimental data. Although S2 and S4 exhibit slightly different backbone conformations, a better fit of the side chain nOes is obtained in both cases: a disappears and furthermore the intensities of b and b* (Hβ-D-Tyr 2–NH-D-Asn 3), above the noise level in fig. 1, are reduced by this averaging.

This first example is clear evidence of the usefulness of NOESY map reconstruction in side chain conformational analysis: first, distance information involving nearest-neighbour residues resolves the intra-residue ambiguities (mainly ascribed to assignment problems); and second, the possible occurrence of local internal flexibility can be determined by triangulation of the various distances. In view of the short Hβ-Hβ distance (1.78 Å), a rigorous computation is required, because all the pieces of information used for determining the molecular topology in fact rely on larger distances, estimates of which may be strongly influenced by the multi-spin effects.

4.2. The interaction of the D-Tyr 2 ring with the D-Ser 6 side chain

Due to the small size of the lipopeptide, all ^{1}H resonances (except those of the hydrophobic tail) have been assigned and a reasonable conformational analysis should provide an explanation for each cross-peak present or absent in the experimental 2D NOESY map. The degree of confidence in both assigning and quantifying each peak will obviously decline as one proceeds from the strongest to the weakest peaks. However, the main problem in the refinement of a conformation using experimental data is basically that of finding a suitable relative weight for each piece of information. Unfortunately, this requirement is quite hard to meet, since long-range nOes may be very important clues in the structure despite their poor confidence level. In contrast to sequential nOes, their reliability cannot be ascertained by the redundancy of some connectivities.

For example, the weak cross-peak observed in fig. 1 at $(\omega_1, \omega_2) = (4.4, 7.2$ ppm), assigned to $C_{2,6}$H protons of D-Tyr 2 and one Hβ of D-Ser 6, is the only evidence that the structure pinches together at D-Tyr 2 and D-Ser 6 to form a horseshoe shape. Reconstructing the S2 map convinces one that peak 'd' is not an artifact due to multi-spin effects. In this map, where most of the data are in agreement with the experiment, no path via a third spin can be found to provide an indirect link between D-Tyr 2 and D-Ser 6 side chains.

In S4, the cross-peak d is below the plot threshold because the horseshoe-like conformation is somewhat relaxed to obtain a better fit of other distance constraints: the corresponding distance is 3.2 Å instead of 2.9 Å in S2. At this point, it should be recalled that the diameter of the circle in the computed maps is a visual description of the nOe effects (without regard to the line width), whereas the NOESY cross-peaks, as shown in a 2D contour plot, reflect intensities but not integrals. In fact, the resonances of the tyrosyl ring are narrower than others due to a higher mobility, which could account for the difference between the experimentally detected NOESY cross-peak d and the weak computed nOe corresponding to a relatively large internuclear distance. The equal line width assumption (see section 3) obviously fails in this case.

4.3. The orientation of the L-Asn 7–β amino acid 8 amide plane

Because both NH and C=O may be involved in hydrogen bonds, their orientation is of great im-

portance in understanding the conformational energy. As a matter of fact, each amide plane can be tilted by a concerted change of ψ_i and ϕ_{i+1} without greatly altering the rest of the cyclic peptide fold. However, the amide plane orientation can be determined only indirectly through several probes (^3J, $d(H_i^\alpha - NH_{i+1})$, $d(NH_i - H_i^\alpha)$, ...[8]). Reconstruction of the NOESY map is the only comprehensive method for checking all this interrelated information.

In a cross-section of the 125 ms NOESY map taken through the chemical shift of the β amino acid 8 NH, no cross-peak stands out from the noise between 2 and 6 ppm. One is therefore forced to answer the question as to whether a conformation can be found, in which this NH has no through-space neighbour within 4.5 Å. This unusual requirement cannot be met fully in either S2 or S4, although the amide plane undergoes a large rotation on going from S2 to S4. The satisfactory fit for the intensity of cross-peak c (assigned to the NH 8-Hα7) in S2 but not in S4 might prompt us to conclude that the amide plane exhibits the correct orientation in S2. However, this hasty conclusion has to be re-examined in view of peaks e and e* assigned to connectivities with the Hβ of L-Asn 7 (fig. 3). Here again, all spectral outcomes of a given optimized structure can be brought to light by the NOESY map reconstruction, leading to the definite conclusion that S2 does not fit better than S4.

Careful inspection of the S2 and S4 map provides guidelines for further improvement of either structure: in view of the intensities of e and e*, efforts can be devoted to their reduction by a rotation of the L-Asn 7 side chain. If this ends in failure, the striking lack of close neighbours for NH β amino acid 8 could also be tentatively explained by means of an equilibrium between two conformations with different orientations of the amide plane (one similar to S2, the other similar to S4). Indeed, this plane turns out to be the only one in mycosubtilin for which all optimization runs do not converge towards a topologically similar conformation. Molecular dynamics simulations performed on globular proteins [23, 24] have revealed independently that even in wellstructured polypeptide chains, the 180° flipping of an amide plane is a likely event (over a range of several tens of picoseconds) but will only perturb its nearest-neighbour atoms.

5. Conclusion

Modelling and refinement of conformations from 2D NMR data are based on knowledge of a set of internuclear distances, introduced as constraints in an energy optimization. The degree of refinement of the final conformation depends on the following factors: (i) the accuracy of measuring the experimental nOe build-up rates, (ii) the accuracy of converting nOes into interproton distances, (iii) the uniqueness of the result of the optimization process (local minima).

In most cases, one obtains a conformation satisfying the experimental constraints to a greater or lesser extent. We have shown that the best way to check the validity of the structure is by simulation of the corresponding 2D NOESY map. The method reported here, which takes into account multi-spin effects, provides a description of the cross-relaxation rates for a rigid molecule without any approximation. Thus, the only limitation is the possiblility of internal flexibility, one that is obviously shared by all techniques used in conformational analysis, including molecular dynamics methods, which fail to describe slow motions (> 500 ps) [25].

Nevertheless, the comparison of an experimental with a computed map is extremely profitable: it reveals local details and therefore provides guidelines for further refinement. It also displays all inconsistencies in the assignment and provides a check afterwards on all interproton distances which were not included in previous steps. With improved reliability of the cross-peak assignment, triangulation techniques allow one to localize more flexible parts of the molecule, in which averaged distances were in fact measured.

The present work is the first step in developing a general method for 2D NOESY map simulation, including secondary features such as ^3J couplings and line shapes. Our final aim is to build an interface between NMR and optimization, in order to reduce errors and misinterpretations by making the process as objective as possible.

References

1 M.P. Williamson, D. Marion and K. Wüthrich, J. Mol. Biol. 173 (1984) 341.
2 M.P. Williamson, T.F. Havel and K. Wüthrich, J. Mol. Biol. 182 (1985) 295.
3 G.M. Clore, A.M. Gronenborn and L.W. McLaughlin, Eur. J. Biochem 151 (1985) 153.
4 D.R. Hare and B.R. Reid, Biochemistry 25 (1986) 5341.
5 D.R. Hare, L. Shapiro and D.J. Patel, Biochemistry 25 (1986) 7445, 7456.
6 A.D. Kline, W. Braun and K. Wüthrich, J. Mol. Biol. 189 (1986) 377.
7 S.L. Gordon and K. Wüthrich, J. Am. Chem. Soc. 100 (1978) 7094.
8 M. Billeter, W. Braun and K. Wüthrich, J. Mol. Biol. 155 (1982) 321; K. Wüthrich, M. Billeter and W. Braun, J. Mol. Biol. 180 (1982) 715.
9 F. Peypoux, G. Michel and L. Delcambe, Eur. J. Biochem. 63 (1976) 391.
10 F. Peypoux, M.T. Pommier, D. Marion, M. Ptak, B.C. Das and G. Michel, J. Antibiot. 39 (1986) 636.
11 S. Macura and R.R. Ernst, Mol. Phys. 41 (1980) 95.
12 D. Marion and K. Wüthrich, Biochem. Biophys. Res. Commun. 113 (1983) 967.
13 D. Marion, M. Genest, A. Caille, F. Peypoux, G. Michel and M. Ptak, Biopolymers 25 (1986) 153.
14 B.P. Roques, R. Rao and D. Marion, Biochimie 62 (1980) 753.
15 D.E. Woessner, J. Chem. Phys. 42 (1965) 1855.
16 D.E. Woessner, J. Chem. Phys. 37 (1962) 647.
17 L.G. Werbelow and D.M. Grant, in: Advances in magnetic resonance, vol. 9, ed. J.S. Waugh (Academic Press, New York, 1977).
18 J.W. Keepers and T.L. James, J. Magn. Reson. 57 (1984) 404.
19 W.H. Press, B.P. Flannery, S.A. Teukolsky and W.T. Vetterling, Numerical recipes – The art of scientific computing (Cambridge University Press, Cambridge, 1986), ch. 11.
20 M. Genest, D. Marion, A. Caille and M. Ptak, Eur. J. Biochem. 169 (1987) 389.
21 K.G.R. Pachler, Spectrochim. Acta 20 (1964) 581.
22 J. Kobayashi, T. Higashijima, S. Sekido and T. Miyazawa, Int. J. Peptide Protein Res. 17 (1981) 486.
23 J.A. McCommon, B.R. Gelin and M. Karplus, Nature 267 (1977) 585.
24 M. Levitt J. Mol. Biol. 168 (1983) 621.
25 R. Kaptein, E.R.P. Zuiderweg, R.M. Scheek, R. Boelens and W.F. van Gunsteren J. Mol. Biol. 182 (1985) 179.